DOI:
10.1016/j.freeradbiomed.2015.12.013

Document Version
Peer reviewed version

Bach1 differentially regulates distinct Nrf2-dependent genes in human venous and coronary artery endothelial cells adapted to physiological oxygen levels

Sarah J. Chapple, Thomas P. Keeley, Daniela Mastronicola, Matthew Arno, Gema Vizcay-Barrena, Roland Fleck, Richard C.M Siow, Giovanni E. Mann

PII: S0891-5849(15)01166-1
DOI: http://dx.doi.org/10.1016/j.freeradbiomed.2015.12.013
Reference: FRB12691

To appear in: *Free Radical Biology and Medicine*

Received date: 14 October 2015
Revised date: 11 December 2015
Accepted date: 12 December 2015

Cite this article as: Sarah J. Chapple, Thomas P. Keeley, Daniela Mastronicola, Matthew Arno, Gema Vizcay-Barrena, Roland Fleck, Richard C.M Siow and Giovanni E. Mann, Bach1 differentially regulates distinct Nrf2-dependent genes in human venous and coronary artery endothelial cells adapted to physiological oxygen levels, *Free Radical Biology and Medicine,* http://dx.doi.org/10.1016/j.freeradbiomed.2015.12.013

Bach1 differentially regulates distinct Nrf2-dependent genes in human venous and coronary artery endothelial cells adapted to physiological oxygen levels

Sarah J. Chapple[1], Thomas P. Keeley[1], Daniela Mastronicola[1]§, Matthew Arno[2], Gema Vizcay-Barrena[3], Roland Fleck[3], Richard C.M Siow[1], Giovanni E. Mann[1]*

1Cardiovascular Division, British Heart Foundation Centre of Research Excellence, Faculty of Life Sciences & Medicine, King's College London, 150 Stamford Street, London SE1 9NH, U.K.

[2]Genomics Centre, King's College London, 150 Stamford Street, London SE1 9NH, U.K.

[3]Centre for Ultrastructural Imaging, King's College London, London SE1 9NH, U.K

Running Title: Normoxia represses select Nrf2 target genes via Bach1

Key Words Endothelial cells; Coronary artery; Physiological Oxygen Tension; Normoxia; Redox Signaling; Nuclear Factor-E2-Related Factor 2, Nrf2; Bach1; HO-1; NQO1; GCL; glutathione reductase GR; Glutathione; Solute Carrier Family 7 - anionic amino acid transporter light chain xCT; thioredoxin reductase-1; Sequestosome-1; Mitochondria

§ Present address: Department of Biochemical Sciences & Instituto Pasteur - Fondazione Cenci Bolognetti, Sapienza University of Rome, Italy

*To whom correspondence should be addressed:

Prof. G.E. Mann, British Heart Foundation Centre of Research Excellence, Faculty of Life Sciences & Medicine, King's College London, 150 Stamford Street, London SE1 9NH, U.K.
E-mail: giovanni.mann@kcl.ac.uk; Tel: +44(0)20 7848-4306

Abstract

The effects of physiological oxygen tension on Nuclear Factor-E2-Related Factor 2 (Nrf2)-regulated redox signaling remain poorly understood. We report the first study of Nrf2-regulated signaling in human primary endothelial cells (EC) adapted long-term to physiological O_2 (5%). Adaptation of EC to 5% O_2 had minimal effects on cell ultrastructure, viability, basal redox status or HIF1-α expression. Affymetrix array profiling and subsequent qPCR/protein validation revealed that induction of select Nrf2 target genes, HO-1 and NQO1, was significantly attenuated in cells adapted to 5% O_2, despite nuclear accumulation and DNA binding of Nrf2. Diminished HO-1 induction under 5% O_2 was stimulus independent and reversible upon re-adaptation to air or silencing of the Nrf2 repressor Bach1, notably elevated under 5% O_2. Induction of GSH-related genes xCT and GCLM were oxygen and Bach1-insensitive during long-term culture under 5% O_2, providing the first evidence that genes related to GSH synthesis mediate protection afforded by Nrf2-Keap1 defense pathway in cells adapted to physiological O_2 levels encountered *in vivo*.

Abbreviations

Bach1	BTB and CNC homology 1, basic leucine zipper transcription factor 1
DJ-1	Parkinson disease-associated protein

EC	Endothelial cells
GCL	Glutamate cysteine ligase
GCLM	Glutamate cysteine ligase modulatory subunit
HCAEC	Human coronary artery endothelial cells
HO-1	Heme oxygenase-1
HUVEC	Human umbilical vein endothelial cells
Nrf2	Nuclear Factor-E2-Related Factor 2
NQO1	NAD(P)H quinone oxidoreductase 1
Keap1	Kelch-like ECH-associated protein 1
xCT	Solute carrier family 7 - anionic amino acid transporter light chain

Introduction

The Nrf2 (NF-E2-related factor 2)/Keap1 (Kelch-like ECH-associated protein 1) pathway plays key role in cellular defenses against oxidative and environmental stress [1-4]. As a redox sensitive transcription factor, Nrf2 regulates endogenous antioxidant defenses, phase II metabolism, autophagy [5] and solute transporters [6]. Nrf2 is increasingly becoming recognised as a therapeutic target for the treatment of chronic diseases associated with oxidative stress [3, 4, 7-9]. The molecular mechanisms regulating Nrf2 signaling have predominantly been investigated *in vitro* using cell culture models exposed to atmospheric oxygen and identified multiple regulatory proteins which repress (Keap1, Bach1) or enhance (DJ-1, p62) Nrf2 activity [3, 4, 10]. As Nrf2 is activated under conditions of hypoxia (<1% O_2) and hyperoxia [11-13], we investigated the regulatory mechanisms and downstream Nrf2 gene targets in human primary endothelial cells (EC) following long-term adaptation to physiological oxygen (5% O_2).

In vivo endothelial (EC) and other cell types reside in a physiological O_2 environment, ranging from to ~3-13%, while in culture cells are normally exposed to atmospheric O_2 levels (20.86% O_2 = 158 mmHg) [14]. Alterations in O_2 tension modulate cell function by affecting intracellular NAD(P)H levels, protein kinases, ion channels and antioxidant defenses [14-18]. Although studies in primary lymphocytes elegantly highlight the importance of studying cellular responses under physiological O_2 (5%) [19-21], the majority of studies have characterized signal transduction in cells cultured in ambient air, with only a few comparing responses after short-term adaptation to different O_2 tensions [13, 20, 22, 23].

The present study provides the first detailed characterization of Nrf2-regulated redox signaling in human primary venous and arterial EC adapted long-term (5 days – 2 weeks) to physiological oxygen (5% O_2). Critically, our study using an O_2-regulated workstation circumvented problems associated with re-oxygenation, enabling us to compare effects of short-term (24 h) versus long-term (5-14 days) adaptation to 5% O_2. A cell-penetrating phosphorescence, O_2-sensitive nanoparticle probe [24, 25] enabled us to monitor real-time changes in cytosolic O_2 content. Using an Affymetrix array, we established that electrophilic stress induces Nrf2 signaling, with glutathione (GSH)-related genes insensitive to changes in O_2 tension. Although Nrf2 nuclear translocation was unaffected by physiological O_2 (5%), induction of select Nrf2 target genes (HO-1, NQO1) was diminished. We further report that basal expression of the Nrf2 repressor Bach1 is elevated in human umbilical vein (HUVEC) and coronary artery (HCAEC) EC adapted to 5% O_2.

Knockdown of Bach1 restored HO-1 induction in EC cultured under 5% O_2 but had negligible effects on basal and electrophile induced GCLM expression, suggesting that under physiological O_2 levels encountered *in vivo* GSH-related genes transduce Nrf2-mediated cellular protection. Thus, investigating redox signaling in cells adapted long-term to physiological O_2 tension provides valuable insights for endothelial metabolism [26] and more importantly bench-to-bedside translation in cardiovascular and regenerative medicine [22, 27].

Materials and Methods

Reagents

Cell culture media, chemicals and reagents were obtained from Sigma-Aldrich (Dorset, UK) unless stated otherwise. Nucleospin 96 RNA Kit was from Macherey-Nagel (Duren, Germany), High Capacity cDNA conversion kit from Applied Biosystems (Paisley, UK), SensiMix SYBR No-Rox PCR Kit from Bioline (London, UK), TransAM nuclear extraction and Nrf2 binding activity assay kit from Active Motif (Carlsbad, USA). Fluorescent superoxide indicator MitoSOX red (M36008) was from Invitrogen Molecular Probes (Carlsbad, USA). Antibodies against Nrf2 (SC-722, mol. wt. 110 kDa band), NQO1 (SC-16464), Lamin A/C (SC-6254), Bach-1 (SC-14700) from Santa Cruz (USA), Keap1 (D6B12, #8047) and DJ-1 (#2134) from Cell Signaling (Massachusetts, USA), HO-1 (ab13243) and NFκB/p65 (ab16502) from Abcam Cambridge, UK), HIF-1α (NB100-449) from Novus Biologicals (Abingdon, UK), α-tubulin (mab1864) and HRP-conjugated secondary goat anti-rabbit (AP132P), goat anti-rat (AP136P) and donkey anti-goat (AP234P HRP) secondary antibodies from Millipore (Billerica, USA). GCLM was a gift from Prof. Terrance J. Kavanagh (University of Washington, USA). Firefly luciferase/luciferin reaction mixture (FLE250) was from Sigma-Aldrich. Human coronary artery endothelial cells (HCAEC) were provided by PromoCell GmbH, Germany.

Endothelial cell culture under defined O_2 levels

Primary human umbilical vein endothelial cells (HUVEC) were cultured in M199 containing 10% fetal calf (FCS) and 10% newborn calf serum [28]. An endothelial phenotype was confirmed by a characteristic cobblestone morphology and positive immunostaining for von Willebrand factor and eNOS which was not altered during culture in 5% O_2 (data not shown). HUVEC and human coronary artery EC (HCAEC) were cultured in a standard incubator gassed with 5% CO_2 in air or an O_2-regulated workstation (Sci-tive, Baker-Ruskinn Company, Maine, USA) gassed with 5% O_2, 5% CO_2, 90% N_2 (75% humidity) with subculture and all treatments conducted within the workstation. All culture media were pre-equilibrated in either ambient air, 5% O_2 or 1% O_2 in the Sci-tive workstation prior to experimentation. Endothelial cells (passage 1-3) were pre-adapted to 5% O_2 for 1 or 5 days, unless stated otherwise. HUVEC were equilibrated in M199 containing 20% serum (-ECGS) for 24 h before treatment for a further 0-24 h with medium alone or containing diethylmaleate (DEM, 100μmol.L^{-1}), 4-hydroxynonenal (HNE, 20μmol.L^{-1}), sulforaphane (SFN, 2.5μmol.L^{-1}) or the NO donor (DETA NONOate, 500μmol.L^{-1}). HCAEC (Promocell C-12221, Germany) were pre-equilibrated in ECM (-growth factors, Promocell C-22020, Germany). For transfection, Bach1 or Nrf2 knockdown was achieved by transfecting HUVEC with 40pmol/24 well scramble, Bach1 or Nrf2 siRNA (Santa Cruz Biotechnology) for 24 h, using DharmaFECT 4 (Thermo Fisher, UK), as per the manufacturer's recommendations, before treatment of EC with DEM (100μmol/L) for 24 h.

Phosphorescence lifetime quantification of O_2 content in endothelial cytosol and medium

Intracellular O_2 levels were measured using a cell-penetrating phosphorescence platinum-porphyrin based nanoparticle probe, MitoXpress®-INTRA (Luxcel Biosciences, Cork, Ireland) [24, 25] and a time-resolved fluorescence plate reader (FLUOstar Omega, BMG Labtech, UK) equipped with an atmospheric control unit, allowing for measurement of cytosolic O_2 content under defined O_2 levels. HUVEC were seeded at 50,000 cells/well in 96-well black microtitre plates and loaded after 48 h by incubation with MitoXpress®-INTRA (10µg.mL^{-1}) for 18 h in M199 containing 20% serum.

Oxygen quenches the phosphorescent emission from MitoXpress®-INTRA, such that phosphorescence measured at 360 nm_{ex} and 655 ± 55 nm_{em} is inversely proportional to [O_2]. Phosphorescence intensity was measured at two delay times (30µs/t_1 and 70µs/t_2) and converted to phosphorescence lifetime (τ) using the following formula: $\tau=(t_2-t_1)/\ln(f_1/f_2)$, where $f_{1/2}$ represents the intensity at $t_{1/2}$. Calibration of phosphorescence lifetime to O_2 concentration (%) was achieved by treating cells with the mitochondrial complex III inhibitor antimycin-A (10µmol.L^{-1}), thereby eliminating any O_2 gradient between the medium and cytosol. Stepwise reductions in ambient O_2 levels were performed (21, 18, 13.5, 10, 7.5, 5, 2 and 1% O_2, with glucose (20 mmol.L^{-1})/glucose oxidase (50µg.ml^{-1}) used to create 0% O_2 levels) and probe lifetime monitored as described in Fig. S 1 A and D. Results were plotted against the applied ambient O_2 tension and subjected to exponential fit analysis, with unknown lifetimes subsequently interpolated from this curve. Dissolved O_2 in the medium was measured in parallel by diluting MitoXpress®-INTRA (2.5µg.mL^{-1}) in medium. Detailed validation of MitoXpress®-INTRA for measurement of O_2 content in primary EC, including all calibration functions and cell viability indices are provided in Fig. S 1.

Impedance measurements of cell adhesion and proliferation

HUVEC were cultured in air or adapted to 5% O_2 for 5 days and then seeded at 20,000 cells.mL^{-1} into iCELLigence 8-well E-plates (E8, ACEA Biosciences Inc., USA). Real-time bioimpedance measurements were obtained using a cell analyser platform (iCELLigence, ACEA Biosciences Inc., USA) [29] maintained at 37°C in air or 5% O_2 within the O_2-regulated workstation. Changes in bioimpedance generated by cell coverage over the electrode in each well of the E8 plates was used to assess cell proliferation and expressed as Cell Index (CI), calculated from the difference between cell and background impedance (see Fig. S2 C). Proliferation was also assessed by monitoring cell protein content present in 0.5M NaOH solubilised extracts (see Fig. S2 B).

Measurement of mitochondrial reactive oxygen species generation

Mitochondrial reactive oxygen species generation was measured using the mitochondrial targeted probe MitoSox red, which we have previously shown is inhibited by PEG-SOD and rotenone in HUVEC [28]. HUVEC, cultured in air or adapted for 1 or 5 days to 5% O_2, were loaded in serum-free M199 with MitoSOX red (5µmol.L^{-1}) for 20 min before treatment for 30 min in the absence or presence of 2µmol.L^{-1} antimycin-A. Fluorescence (Ex 545nm/Em 602nm) was detected in 4% paraformaldehyde fixed cells using a Nikon Diaphot microscope, with images captured using an ORCA-03G (Hamamatsu, Japan) camera with 0.89s exposure. All fluorescence quantification was conducted using uncorrected or contrast images (Fig. S2 D). For enhanced print quality, representative cell fluorescence images shown in Fig. S3 were contrast adjusted

equally. Corrected total fluorescence units (CTFU) from 3-4 fields of view for each condition were quantified by densitometry using Image J, with background and cell area correction applied (Cell integrated density-(cell area*background)).

Transmission electron microscopy

HUVEC were cultured in air or adapted to 5% O_2 for 5 days in M199 + 20% serum and then fixed in 2.5% glutaraldehyde/0.1M cacodylate buffer for 4 h at room temperature. Cells were washed twice in buffer before osmification in 1% OsO_4 in 0.1M cacodylate buffer for 1 h at room temperature, and twice with dH_2O. En bloc staining was conducted using 1% uranyl acetate (UA) aqueous for 1h at room temperature before 5 further washes and sample dehydration using sequential ethanol washes (70% ethanol 10min; 90% ethanol 10min; 100% ethanol 3 x 15min). Monolayers were embedded in epoxy resin and cured overnight at 70°C. Ultrathin sections were stained with uranyl acetate and lead citrate before obtaining EM images using a FEI Tecnai 12 transmission electron microscope operated at 120 kV. Images were acquired with an AMT 16000M digital camera (Fig. S2 E).

Affymetrix mRNA microarrays in HUVEC adapted to air or 5% O_2

HUVEC cultured in air or adapted to 5% O_2 for 5 days were treated for 4 h with M199 alone or containing diethylmaleate (DEM, 100µmol.L^{-1}), a well characterized electrophilic activator of Nrf2 [1] known to induce oxidation of Cys151 on Keap1 and deplete intracellular glutathione [30-32]. Cells were lyzed in Qiazol before extraction of total RNA using a mRNeasy minikit (Qiagen) and fractions used for gene expression analysis by Affymetrix Human Transcriptome 2.0 (HTA 2.0) GeneChip array. Chip processing and data handling was in accordance with the manufacturers guidelines. Total RNA (250ng) from HUVEC, cultured in air or adapted to 5% O_2 for 5 days, was processed and labeled using WT PLUS reagent kit (Affymetrix) and hybridised to Human Transcriptome 2.0 (HTA 2.0) GeneChip array (Affymetrix) [33]. Arrays were processed and scanned following the manufacturer's instructions and using GeneChip Fluidics Station FS450 and GCS3000 7G scanner. Raw data (CEL files) were processed in Expression Console software using the RMA algorithm for normalization, background correction and summarization at the gene levels. Principal Component Analysis (PCA) was used (Omics Explore, Qlucore AB, Sweden) to visualise independent HUVEC cultures, providing a multidimensional representation of samples in three dimensions, with each dimension consisting of a signature of probes/variables with a similar pattern across the samples. These components were ranked by the percentage of the variability they represent. Despite donor variability, two groups of samples (control and DEM in EC adapted to air) were clearly separated from each other along the axis of main principal component. Using the Affymetrix Transcriptome Analysis Console, molecules from the data set that met the basal/DEM ratio cutoff of >1.2 or <-1.2 and P cut-off of <0.05 (q0.2 air q0.5 5% O_2) were used to generate gene lists of DEM-responsive genes and mapped to the relevant canonical pathways.

Nrf2 Binding to ARE using TransAM assay

HUVEC cultured in air or adapted to 5% O_2 for 1 or 5 days were treated for 2 h with control medium alone or containing DEM (100µmol.L^{-1}) and nuclear proteins extracted (Active Motif) according to the manufacturer's instructions, as previously described [7]. The binding activity of nuclear Nrf2 to ARE (5'-GTCACAGTGACTCAGCAGAATCTG-3') was determined by ELISA (TransAM Nrf2 kit, Active Motif).

Immunoblotting

Whole cell lysates were extracted with SDS lysis buffer (containing protease and phosphatase inhibitor cocktails, pH 6.8) on ice for 10min [7, 28]. Nuclear protein was extracted using a nuclear extraction kit (Active Motif). Denatured samples (10µg) were separated by gel electrophoresis, electro-transferred onto polyvinylidene difluoride membranes, and then probed with primary and HRP-conjugated secondary antibodies, using α-tubulin and lamin C as reference proteins for whole cell and nuclear protein, respectively [7]. Protein expression was determined by enhanced chemiluminescence with images captured in a gel documentation system (G-BOX, Syngene Ingenius Bioimaging) and densitometry performed using Image J software (National Institute of Health, USA). As specified in the legend to Fig. 3, lanes were spliced to adjust the lane sequence.

Quantitative RT-PCR (qPCR)

HUVEC were cultured in air or adapted to 5% O_2 for 1 or 5 days, treated for 4 h with M199 alone or containing diethylmaleate (DEM, 100µmol.L^{-1}) and RNA isolated using a Nucleospin RNA Kit (Macherey-Nagel). A spectrophotometer (NanoDrop, Thermo Scientific, UK) was used to assess sample RNA content and purity. Total RNA was reverse–transcribed using a high capacity cDNA conversion kit (Applied Biosystems) and NQO1, HO-1, GCLM, Nrf2, Keap1 and xCT mRNA assessed by real-time qPCR (Corbett Rotorgene) [7]. mRNA expression was normalized to the geometric mean of ß-2-microglobulin (B2M), ribosomal protein L13a (RPL13A) and succinate dehydrogenase unit complex A (SDHA) and primer sequences are listed in Table S1.

Measurement of intracellular glutathione and ATP levels

HUVEC, cultured in air or adapted for 1 or 5 days to 5% O_2, were extracted for glutathione (GSH) with 6.5% trichloroacetic acid on ice for 10 min, and total cellular GSH measured using a fluorometric assay [7]. ATP content was determined using a Firefly luciferase/luciferin reaction mixture for acid extracts of samples or ATP standards (0 to 40nmol.L^{-1}). Bioluminescence was measured for 10 s in a microplate reader (BMG Labtech) [34].

Statistical analysis

Data denote mean ± S.E.M. of measurements in independent cultures from n = 3-12 different donors. Statistical analyses were conducted using a Student's t-test or two-way ANOVA followed by Bonferroni's multiple comparisons, with $P<0.05$ considered significant.

Results

Affymetrix mRNA profiling reveals diminished Nrf2 target gene induction in HUVEC adapted to physiological O_2 levels

A preliminary global transcriptome analysis of HUVEC cultured in air or adapted to 5% O_2 for 5 days, revealed that diethylmaleate (DEM, 100µmol.L^{-1}) induced 564 coding transcripts in air, with Nrf2 the pre-dominant pathway activated, including antioxidant (heme oxygenase-1, HO-1) and phase II (glutathione reductase, thioredoxin reductase-1, NAD(P)H quinone oxidoreductase 1), GSH-related (glutamate-cysteine ligase, Solute Carrier Family 7 - anionic amino acid transporter light chain, xCT) and metabolic/transporter/autophagy-related (Multidrug Resistance-Associated Protein 4, Phosphogluconate

Dehydrogenase, Sequestosome-1) genes (Fig. 1A, main panel). Gene induction at 5% O_2 was diminished, with 276 coding transcripts induced by DEM and GCLM and xCT the key targets of DEM challenge (Fig. 1A, inset panel). Comparison of air and 5% O_2 basal and DEM responses further indicated that basal and maximal HO-1 induction may be diminished in HUVEC adapted to 5% O_2.

Real-time measurements of medium and intracellular O_2 content confirm exposure of cells to physiological O_2 levels

Previous studies of the effects of O_2 tension on cultured cells have often omitted measurements of the O_2 gradient between the medium and intracellular environment, leading to conflicting reports associated with activation of hypoxia-regulated signaling pathways. In the present study, we have monitored real-time cytosolic O_2 content in EC preloaded with the novel O_2-sensitive nanoparticle probe MitoXpress®-INTRA. To validate our nanoparticle sensor measurements of intracellular O_2 content, we initially investigated the concentration- (5-15 $\mu g.mL^{-1}$) and time- (6-24 h) dependence of nanoparticle loading in HUVEC cultured in air, confirming that raw phosphorescence values increased but did not translate into differences in lifetime due to the ratiometric conversion for lifetime phosphorescence (Fig. S1 A and D). Similarly, intracellular GSH and ATP levels were unaffected in EC loaded for 24 h with the nanoparticle probe during culture in air or 5% O_2 for 5 days (Fig. S1 B and C), confirming cell viability was unaffected by nanoparticle exposure and/or long-term culture under 5% O_2.

Fig. 1B shows the relationship between ambient O_2 levels and cytosolic O_2 content in HUVEC exposed to different O_2 concentrations (0 – 21%) in an O_2-regulated, time-resolved fluorescence plate reader. When EC were maintained under standard culture conditions in air for 60 min and then exposed to 5% O_2, equilibration of cytosolic and medium O_2 content required ~30 min (Fig. 1 B, C). Dissolved O_2 in the medium above the cell monolayer was slightly higher than cytosolic levels (Fig. 1 B, C). When cells were adapted from an air-5% CO_2 to 5% O_2-5% CO_2 gas mixture, intracellular O_2 levels declined from 17.4 ± 0.5% to 3.6 ± 0.1% and were maintained at this level during adaptation over 1 to 5 days. Notably, cells maintained continuously under 5% O_2 achieved a cellular O_2 content of 3.6%, consistent with values reported for the umbilical vein *in vivo* [35]. Under these conditions, activation of HIF-1α was not detected (Fig. S 2 A), and previous reports of HIF-1α activation in EC exposed to a 3% O_2 environment [36] most likely reflect intracellular O_2 levels approaching hypoxia (<2% O_2).

Effects of physiological O_2 on cell adhesion, proliferation and mitochondrial superoxide generation

To characterize the effects of physiological O_2 on the phenotype of EC under basal conditions, we monitored adhesion and proliferation of HUVEC during culture in air 5% O_2 for 5 days, by measuring cell protein content (Fig. S2 B) or using a bioimpedance iCELLigence platform [29] maintained within an O_2-regulated workstation (Fig. S2 C). Proliferation but not adhesion was reduced during culture under 5% O_2, confirming previous observations in primary human venular EC [37] and lymphocytes [19].

To determine the effects of physiological O_2 on the redox state of HUVEC, we assayed MitoSox red fluorescence as an index of mitochondrial reactive oxygen species generation. Fluorescence increased transiently after 1 day adaptation to 5% O_2, with inhibition of mitochondrial complex III by antimycin A leading to similar increases in superoxide generation in HUVEC cultured in air or 5% O_2 for 1 or 5 days

(Fig. S2D and Fig. S3). The transient increase in superoxide generation is consistent with a previous report of increased dihydroethidine oxidation in HUVEC exposed acutely (1 h) to 3% O_2 [38]. Long-term adaptation of HUVEC to 5% O_2 had no effect on protein carbonylation or basal expression of SOD2, catalase or eNOS (data not shown), and transmission electron microscopy confirmed that 5-day adaptation to 5% O_2 had negligible effects on cell morphology (see Fig. S2 E), with an absence of organelle swelling/distention or loss of parallel double membranes surrounding in the nuclear envelope, endoplasmic reticulum (ER) or mitochondria.

Physiological O_2 has no effect on Nrf2 nuclear translocation although induction of target genes HO-1 and NQO1 is diminished

To further validate whether long-term adaptation to 5% O_2 affects Nrf2 signaling, we examined the effects of physiological O_2 (5%) on Nrf2 DNA binding capacity and the induction of key downstream targets by real time qPCR and immunoblotting. Activation of Nrf2 by DEM (100µmol.L^{-1}), a classical stimulus known to induce oxidation of Cys151 on Keap1[31], was assessed by nuclear Nrf2 accumulation (Fig. 2 A) and Nrf2 *in vitro* DNA binding activity (Fig. 2 B). Notably, Nrf2 activation was similar in EC cultured in air or adapted to 5% O_2 for 1 or 5 days. In contrast, protein and mRNA expression of the Nrf2 target genes HO-1 (Fig. 3 A and B) and NAD(P)H quinone oxidoreductase 1 (NQO1, Fig. 3 C and D) induced by DEM were attenuated in HUVEC adapted to 5% O_2, consistent with a previous report in the murine RAW264.7 macrophage cell line [39]. Notably, attenuation of DEM stimulated HO-1 expression in HUVEC adapted to 5% O_2 was fully reversible on re-adaptation of cells to air for 5 days (Fig. 3 E), indicating phenotypic plasticity. To confirm whether attenuated HO-1 induction in HUVEC adapted long-term to 5% O_2 was stimulus specific, we investigated the effects of other known Nrf2 activators. Treatment of HUVEC for 12 h with the lipid peroxidation product 4-hydroxynonenal [40] (Fig. 4 A), the isothiocyanate sulforaphane [8] (Fig. 4 B) or the nitric oxide donor DETA NONOate [41] (Fig. 4 C) led to a marked induction of HO-1 in HUVEC cultured in air, which was significantly attenuated in cells adapted to 5% O_2 for 1 or 5 days. Studies in human coronary artery EC (HCAEC), adapted to 5% O_2 for 5 days and then challenged with 4-hydroxynonenal (12 h, 20µmol.L^{-1}) (Fig. S 4), confirmed our findings of attenuated HO-1 and NQO1 induction in primary venous EC.

Adaptation to physiological O_2 upregulates expression of Bach1, a repressor of HO-1 and NQO1

BTB and CNC homology 1, basic leucine zipper transcription factor 1 (Bach1) lacks transcriptional activity and acts as a negative regulator of HO-1 and NQO1 gene transcription [42] by binding Maf recognition elements [43]. Notably, prolonged hypoxia (1% O_2) has been shown to upregulate Bach1 expression in HUVEC and other cell types [12]. We here report the first evidence that adaptation of HUVEC to physiological O_2 tension (5%) for 1 or 5 days upregulates Bach1 protein (24 h) and mRNA (4 h) expression (Fig. 5 A and B) independent of HIF-1α induction (Fig. S 2A), with similar findings obtained for Bach1 protein expression in HCAEC (Fig. S 4 C). siRNA knockdown of Bach1 in HUVEC adapted to 5% O_2 restored diethylmaleate stimulated HO-1 expression (Fig. 5 C) to levels observed in EC adapted to air (see Fig. 3).

When we further examined whether adaptation of EC to physiological O_2 affects other modulators of

Nrf2 signaling, such as Keap1 (cytosolic binding protein for Nrf2) [2] and DJ-1 (Parkinson disease-associated protein and stabilizer of Nrf2) [44], basal expression of Keap1 and DJ-1 was unaffected following adaptation of HUVEC to 5% O_2 for 1 or 5 days (Fig. S 5, A and B). Moreover, adaptation of HUVEC to 5% O_2 had negligible effects on NFκB expression (Fig. S 5 C).

Physiological O_2 does not affect GSH synthesis despite elevated Bach1 expression

Stress-induced synthesis of the key intracellular thiol GSH is dependent on Nrf2-regulated cystine-glutamate transporter xCT and GCL activity [6, 45, 46], known to be induced by the electrophilic agent diethylmaleate [30, 47]. We here report that basal and diethylmaleate stimulated intracellular GSH levels were unaffected following adaptation of HUVEC to 5% O_2 for 1 or 5 days (Fig. 6 A). Moreover, adaptation to 5% O_2 had negligible effects on basal and diethylmaleate stimulated expression of the xCT transporter (Fig. 6 B) or GCL modulator subunit (GCLM) (Fig. 6 C), consistent with our Affymetrix transcriptome data.

In cells cultured in air, Bach1 is reported to repress expression of the Nrf2 targets GCLM and xCT [48]. To assess whether elevated Bach1 levels in EC adapted to 5% O_2 affect GCLM expression, HUVEC were transfected with Bach1 siRNA. Notably, unlike restoration of HO-1 expression following Bach1 knockdown (Fig. 5 C), GCLM expression in HUVEC adapted to 5% O_2 was not augmented by knockdown of Bach1 (Fig. 6 D), suggesting that under physiological O_2 GSH synthesis is independent of Bach1. As previous studies in other human cell types cultured in air have reported that GCLM is negatively regulated by Bach1 [48], we conducted further 'control' experiments in HUVEC cultured in air. As shown in Fig. S 6, knockdown of Bach1 in HUVEC cultured in air enhances GCLM expression, confirming previous reports in other human cell types [48]. Collectively, these results suggest that GSH-related genes may mediate transducers ofNrf2-regulated antioxidant defenses under physiological O_2 due to their insensitivity to Bach1 regulation.

Discussion

Our study establishes that the O_2 environment in which endothelial cells are cultured *in vitro* significantly influences inducible but not basal redox defenses regulated by Nrf2. Our findings reveal that adaptation to physiological O_2 (5%) significantly alters the regulation of select Nrf2 targets genes by Bach1. We provide the first evidence that Bach1 is upregulated in human primary endothelial cells adapted long-term to physiological O_2 in the absence of HIF-1α stabilization. Moreover, elevated Bach1 levels regulate a smaller subset of Nrf2 defense genes than those previously identified under standard atmospheric culture conditions [48]. Although the induction of HO-1 and NQO1 is diminished in endothelial cells adapted to 5% O_2, notably GSH levels and expression of GCLM and xCT are unaffected, suggesting that under physiological O_2 levels encountered *in vivo* genes related to GSH synthesis may mediate Nrf2-regulated cellular protection.

The O_2 concentration in the umbilical vein *in vivo* approximates 3.7% [35] and, as blood flow minimizes the formation of significant O_2 gradients, cellular O_2 levels should mimic this level closely. In previous studies, primary HUVEC were adapted long-term to 3% O_2 in an attempt to mimic O_2 levels *in vivo* [36] but, as illustrated in Fig. 1B, this results in a cytosolic O_2 content of ~2% and an hypoxic phenotype characterized by enhanced HIF-1α and target gene expression [36]. Moreover, use of O_2-regulated workstations and plate

readers has enabled us to study cells under defined O_2 tension, obviating oxidative stress induced by reoxygenation during routine cell culture. We employed an O_2-sensitive nanoparticle probe to demonstrate that O_2 content in EC decreases as dissolved O_2 in the culture medium is lowered from 18% to 5% O_2, and confirmed an intracellular O_2 content of 3.6% in HUVEC adapted long-term to 5% O_2. Although upregulation of HIF-1α in EC exposed to hypoxia decreases Nrf2-driven luciferase and HO-1 expression [49], the cytosolic O_2 level (3.6%) achieved in our experiments after 5 days adaptation of HUVEC to 5% O_2 did not increase HIF-1α protein levels (Fig. S 2 A).

Previous studies have shown that changes in O_2 tension can affect the phenotype of cells, resulting from alterations in the activity of ion channels, kinases and redox sensitive genes [14-18]. Despite these reports, our observations concerning basal redox status following long-term adaptation of primary HUVEC to 5% O_2 revealed no effect on protein carbonylation, basal expression of SOD2, catalase or eNOS (data not shown). Furthermore, our EM data reveals negligible changes in cell morphology (Fig. S2 E) following long-term adaptation.

Diminished Nrf2 regulated HO-1 induction under 5% O_2 was agonist independent (Fig. 4) and reversible upon re-adaptation to air, indicating plasticity of redox defenses in human primary venous (Fig. 3) and arterial (Fig. S4) EC adapted to different O_2 tensions. Our experiments suggest that upregulation of Bach1 in primary endothelial cells under physiological O_2 levels may account for the downregulation of HO-1 and NQO1 induction [12, 50] rather than reduced nuclear Nrf2 translocation (Fig. 2). This hypothesis is further supported by our finding that knockdown of Bach1 in endothelial cells adapted to 5% O_2 restores diethylmaleate stimulated HO-1 induction. Increased heme levels are known to inhibit DNA binding of Bach1, enabling transcriptional activators to bind to HO-1 enhancers [42, 51, 52]. Nrf2 has been reported to regulate Bach1 expression [53], however, as we observed no change in Nrf2 activity following adaptation to 5% O_2, it is unlikely that elevated basal Bach1 expression is dependent on Nrf2. In this context, Bach1 has been has been reported to upregulate its own gene expression [54], and as shown in Fig. 5 C and Fig. 6 D siRNA knockdown of Bach1 is highly efficient.

Previous studies in HUVEC established that prolonged hypoxia (1% O_2, 18-48 h) upregulates Bach1 and downregulates HO-1 expression [12]. To our knowledge, the present findings provide the first evidence that long-term adaptation of human venous (HUVEC) or coronary artery (HCAEC) endothelial cells to physiological O_2 (5%) upregulates Bach1 mRNA and/or protein expression. We have not examined whether adaptation to 5% O_2 affects the stability of HO-1 mRNA, however, culture of human endothelial cells (HUVEC, HCAEC or ECV304) under hypoxia (1% O_2) represses HO-1 mRNA expression without affecting mRNA degradation [55].

Fig. 7 illustrates our hypothesis that in human primary endothelial cells under physiological O_2 levels (5% O_2, *'physiological normoxia'*) Nrf2 confers vascular protection mainly via induction of GCLM and the xCT involved in GSH biosynthesis. The insensitivity of GSH-related genes to Bach1 mediated repression provides a mechanism for maintaining endothelial antioxidant defenses under '*physiological normoxia*', despite repression of HO-1 and NQO1 transcription by Bach1. Over the past decades, endothelial cells cultured under 18% O_2/5% CO_2 have been used to characterize the action of vasoactive mediators,

intracellular Ca^{2+} mobilisation, changes in pro- and anti-inflammatory gene expression and Nrf2-regulated genes. Our novel findings highlight the importance of investigating redox signaling in cells adapted to physiological O_2 and provide valuable insights for cardiovascular and regenerative medicine.

Acknowledgements

We acknowledge Prof. Dmitri B. Papkovsky (Biochemistry Department, University College Cork, Ireland), Conn Carey and Dr James Hynes (Luxcel Biosciences Ltd, Cork, Ireland) for their helpful scientific advice and supply of reagents. We thank Prof. Terrance J. Kavanagh (University of Washington, USA) for the GCLM antibody and the Research Midwives at St. Thomas Hospital for collection of umbilical cords. This work was supported by grants from the British Heart Foundation (FS/13/66/30445, PG/13/1/29801) and a Novel and Emerging Technologies Grant from Heart Research UK (NET01/13).

References

[1] Ishii, T.; Itoh, K.; Takahashi, S.; Sato, H.; Yanagawa, T.; Katoh, Y.; Bannai, S.; Yamamoto, M. Transcription factor Nrf2 coordinately regulates a group of oxidative stress-inducible genes in macrophages. *J.Biol.Chem.* **275:**16023-16029; 2000.

[2] Itoh, K.; Wakabayashi, N.; Katoh, Y.; Ishii, T.; Igarashi, K.; Engel, J. D.; Yamamoto, M. Keap1 represses nuclear activation of antioxidant responsive elements by Nrf2 through binding to the amino-terminal Neh2 domain. *Genes Dev* **13:**76-86; 1999.

[3] Suzuki, T.; Yamamoto, M. Molecular basis of the Keap1-Nrf2 system. *Free Radic Biol Med*; 2015.

[4] Tebay, L. E.; Robertson, H.; Durant, S. T.; Vitale, S. R.; Penning, T. M.; Dinkova-Kostova, A. T.; Hayes, J. D. Mechanisms of activation of the transcription factor Nrf2 by redox stressors, nutrient cues, and energy status and the pathways through which it attenuates degenerative disease. *Free Radic Biol Med*; 2015.

[5] Jiang, T.; Harder, B.; Rojo de la Vega, M.; Wong, P. K.; Chapman, E.; Zhang, D. D. p62 links autophagy and Nrf2 signaling. *Free Radic Biol Med*; 2015.

[6] Sato, H.; Tamba, M.; Kuriyama-Matsumura, K.; Okuno, S.; Bannai, S. Molecular cloning and expression of human xCT, the light chain of amino acid transport system xc. *Antioxid Redox Signal* **2:**665-671; 2000.

[7] Cheng, X.; Chapple, S. J.; Patel, B.; Puszyk, W.; Sugden, D.; Yin, X.; Mayr, M.; Siow, R. C.; Mann, G. E. Gestational diabetes mellitus impairs Nrf2-mediated adaptive antioxidant defenses and redox signaling in fetal endothelial cells in utero. *Diabetes* **62:**4088-4097; 2013.

[8] Dinkova-Kostova, A. T.; Kostov, R. V. Glucosinolates and isothiocyanates in health and disease. *Trends Mol Med* **18:**337-347; 2012.

[9] Kanninen, K. M.; Pomeshchik, Y.; Leinonen, H.; Malm, T.; Koistinaho, J.; Levonen, A. L. Applications of the Keap1-Nrf2 system for gene and cell therapy. *Free Radic Biol Med*; 2015.

[10] Komatsu, M.; Kurokawa, H.; Waguri, S.; Taguchi, K.; Kobayashi, A.; Ichimura, Y.; Sou, Y. S.; Ueno, I.; Sakamoto, A.; Tong, K. I.; Kim, M.; Nishito, Y.; Iemura, S.; Natsume, T.; Ueno, T.; Kominami, E.; Motohashi, H.; Tanaka, K.; Yamamoto, M. The selective autophagy substrate p62 activates the stress responsive transcription factor Nrf2 through inactivation of Keap1. *Nat Cell Biol* **12:**213-223; 2010.

[11] Cho, H. Y.; Jedlicka, A. E.; Reddy, S. P.; Zhang, L. Y.; Kensler, T. W.; Kleeberger, S. R. Linkage analysis of susceptibility to hyperoxia. Nrf2 is a candidate gene. *Am J Respir Cell Mol Biol* **26:**42-51; 2002.

[12] Kitamuro, T.; Takahashi, K.; Ogawa, K.; Udono-Fujimori, R.; Takeda, K.; Furuyama, K.; Nakayama, M.; Sun, J.; Fujita, H.; Hida, W.; Hattori, T.; Shirato, K.; Igarashi, K.; Shibahara, S. Bach1 functions as a hypoxia-inducible repressor for the heme oxygenase-1 gene in human cells. *J Biol Chem* **278:**9125-9133; 2003.

[13] Sato, H.; Kuriyama-Matsumura, K.; Hashimoto, T.; Sasaki, H.; Wang, H.; Ishii, T.; Mann, G. E.; Bannai, S. Effect of oxygen on induction of the cystine transporter by bacterial lipopolysaccharide in mouse peritoneal macrophages. *J Biol Chem* **276:**10407-10412; 2001.

[14] Ward, J. P. Oxygen sensors in context. *Biochim Biophys Acta* **1777:**1-14; 2008.

[15] Weir, E. K.; Lopez-Barneo, J.; Buckler, K. J.; Archer, S. L. Acute oxygen-sensing mechanisms. *N Engl J Med* **353:**2042-2055; 2005.

[16] Gupte, S. A.; Wolin, M. S. Relationships between vascular oxygen sensing mechanisms and hypertensive disease processes. *Hypertension* **60:**269-275; 2012.

[17] Knock, G. A.; Ward, J. P. Redox regulation of protein kinases as a modulator of vascular function. *Antioxid Redox Signal* **15:**1531-1547; 2011.

[18] Miura, K.; Ishii, T.; Sugita, Y.; Bannai, S. Cystine uptake and glutathione level in endothelial cells exposed to oxidative stress. *Am J Physiol* **262:**C50-58; 1992.

[19] Atkuri, K. R.; Herzenberg, L. A.; Herzenberg, L. A. Culturing at atmospheric oxygen levels impacts lymphocyte function. *Proc Natl Acad Sci U S A* **102:**3756-3759; 2005.

[20] Atkuri, K. R.; Herzenberg, L. A.; Niemi, A. K.; Cowan, T.; Herzenberg, L. A. Importance of culturing primary lymphocytes at physiological oxygen levels. *Proc Natl Acad Sci U S A* **104:**4547-4552; 2007.

[21] Sahaf, B.; Atkuri, K.; Heydari, K.; Malipatlolla, M.; Rappaport, J.; Regulier, E.; Herzenberg, L. A.; Herzenberg, L. A. Culturing of human peripheral blood cells reveals unsuspected lymphocyte responses relevant to HIV disease. *Proc Natl Acad Sci U S A* **105:**5111-5116; 2008.

[22] Abaci, H. E.; Truitt, R.; Luong, E.; Drazer, G.; Gerecht, S. Adaptation to oxygen deprivation in cultures of human pluripotent stem cells, endothelial progenitor cells, and umbilical vein endothelial cells. *Am J Physiol Cell Physiol* **298:**C1527-1537; 2010.

[23] Pattappa, G.; Thorpe, S. D.; Jegard, N. C.; Heywood, H. K.; de Bruijn, J. D.; Lee, D. A. Continuous and uninterrupted oxygen tension influences the colony formation and oxidative metabolism of human mesenchymal stem cells. *Tissue Eng Part C Methods* **19:**68-79; 2013.

[24] Fercher, A.; Borisov, S. M.; Zhdanov, A. V.; Klimant, I.; Papkovsky, D. B. Intracellular O2 sensing probe based on cell-penetrating phosphorescent nanoparticles. *ACS Nano* **5:**5499-5508; 2011.

[25] Zhdanov, A. V.; Dmitriev, R. I.; Hynes, J.; Papkovsky, D. B. Kinetic analysis of local oxygenation and respiratory responses of mammalian cells using intracellular oxygen-sensitive probes and time-resolved fluorometry. *Methods Enzymol* **542:**183-207; 2014.

[26] Eelen, G.; de Zeeuw, P.; Simons, M.; Carmeliet, P. Endothelial Cell Metabolism in Normal and Diseased Vasculature. *Circ Res* **116:**1231-1244; 2015.

[27] Li, T. S.; Cheng, K.; Malliaras, K.; Matsushita, N.; Sun, B.; Marban, L.; Zhang, Y.; Marban, E. Expansion of human cardiac stem cells in physiological oxygen improves cell production efficiency and potency for myocardial repair. *Cardiovasc Res* **89:**157-165; 2011.

[28] Rowlands, D. J.; Chapple, S.; Siow, R. C.; Mann, G. E. Equol-stimulated mitochondrial reactive oxygen species activate endothelial nitric oxide synthase and redox signaling in endothelial cells: roles for F-actin and GPR30. *Hypertension* **57:**833-840; 2011.

[29] Szabo, C.; Coletta, C.; Chao, C.; Modis, K.; Szczesny, B.; Papapetropoulos, A.; Hellmich, M. R. Tumor-derived hydrogen sulfide, produced by cystathionine-beta-synthase, stimulates bioenergetics, cell proliferation, and angiogenesis in colon cancer. *Proc Natl Acad Sci U S A* **110:**12474-12479; 2013.

[30] Bannai, S. Induction of cystine and glutamate transport activity in human fibroblasts by diethyl maleate and other electrophilic agents. *J Biol Chem* **259:**2435-2440; 1984.

[31] Kobayashi, M.; Li, L.; Iwamoto, N.; Nakajima-Takagi, Y.; Kaneko, H.; Nakayama, Y.; Eguchi, M.; Wada, Y.; Kumagai, Y.; Yamamoto, M. The antioxidant defense system Keap1-Nrf2 comprises a multiple sensing mechanism for responding to a wide range of chemical compounds. *Mol Cell Biol* **29:**493-502; 2009.

[32] Takaya, K.; Suzuki, T.; Motohashi, H.; Onodera, K.; Satomi, S.; Kensler, T. W.; Yamamoto, M. Validation of the multiple sensor mechanism of the Keap1-Nrf2 system. *Free Radic Biol Med* **53:**817-827; 2012.

[33] Furney, S. J.; Pedersen, M.; Gentien, D.; Dumont, A. G.; Rapinat, A.; Desjardins, L.; Turajlic, S.; Piperno-Neumann, S.; de la Grange, P.; Roman-Roman, S.; Stern, M. H.; Marais, R. SF3B1 mutations are associated with alternative splicing in uveal melanoma. *Cancer Discov* **3:**1122-1129; 2013.

[34] Anwar, A. A.; Li, F. Y.; Leake, D. S.; Ishii, T.; Mann, G. E.; Siow, R. C. Induction of heme oxygenase 1 by moderately oxidized low-density lipoproteins in human vascular smooth muscle cells: role of mitogen-activated protein kinases and Nrf2. *Free Radic Biol Med* **39:**227-236; 2005.

[35] Riley, R. J.; Johnson, J. W. Collecting and analyzing cord blood gases. *Clin Obstet Gynecol* **36:**13-23; 1993.

[36] Jiang, Y. Z.; Wang, K.; Li, Y.; Dai, C. F.; Wang, P.; Kendziorski, C.; Chen, D. B.; Zheng, J. Transcriptional and functional adaptations of human endothelial cells to physiological chronic low oxygen. *Biol Reprod* **88:**114; 2013.

[37] Li, R. K.; Shaikh, N.; Weisel, R.; Tumiati, L.; Wu, T. W.; Mickle, D. Cultured vascular endothelial cell susceptibility to extracellularly generated oxidant injury. *J Mol Cell Cardiol* **24:**595-604; 1992.

[38] Quintero, M.; Colombo, S. L.; Godfrey, A.; Moncada, S. Mitochondria as signaling organelles in the vascular endothelium. *Proc Natl Acad Sci U S A* **103:**5379-5384; 2006.

[39] Haas, B.; Chrusciel, S.; Fayad-Kobeissi, S.; Dubois-Rande, J. L.; Azuaje, F.; Boczkowski, J.; Motterlini, R.; Foresti, R. Permanent culture of macrophages at physiological oxygen attenuates the antioxidant and immunomodulatory properties of dimethyl fumarate. *J Cell Physiol* **230:**1128-1138; 2015.

[40] Ishii, T.; Itoh, K.; Ruiz, E.; Leake, D. S.; Unoki, H.; Yamamoto, M.; Mann, G. E. Role of Nrf2 in the regulation of CD36 and stress protein expression in murine macrophages: activation by oxidatively modified LDL and 4-hydroxynonenal. *Circ Res* **94:**609-616; 2004.

[41] Buckley, B. J.; Marshall, Z. M.; Whorton, A. R. Nitric oxide stimulates Nrf2 nuclear translocation in vascular endothelium. *Biochem Biophys Res Commun* **307:**973-979; 2003.

[42] Sun, J.; Hoshino, H.; Takaku, K.; Nakajima, O.; Muto, A.; Suzuki, H.; Tashiro, S.; Takahashi, S.; Shibahara, S.; Alam, J.; Taketo, M. M.; Yamamoto, M.; Igarashi, K. Hemoprotein Bach1 regulates enhancer availability of heme oxygenase-1 gene. *EMBO J* **21:**5216-5224; 2002.

[43] Kimura, M.; Yamamoto, T.; Zhang, J.; Itoh, K.; Kyo, M.; Kamiya, T.; Aburatani, H.; Katsuoka, F.; Kurokawa, H.; Tanaka, T.; Motohashi, H.; Yamamoto, M. Molecular basis distinguishing the DNA binding profile of Nrf2-Maf heterodimer from that of Maf homodimer. *J Biol Chem* **282:**33681-33690; 2007.

[44] Clements, C. M.; McNally, R. S.; Conti, B. J.; Mak, T. W.; Ting, J. P. DJ-1, a cancer- and Parkinson's disease-associated protein, stabilizes the antioxidant transcriptional master regulator Nrf2. *Proceedings of the National Academy of Sciences of the United States of America* **103:**15091-15096; 2006.

[45] Franklin, C. C.; Backos, D. S.; Mohar, I.; White, C. C.; Forman, H. J.; Kavanagh, T. J. Structure, function, and post-translational regulation of the catalytic and modifier subunits of glutamate cysteine ligase. *Mol Aspects Med* **30:**86-98; 2009.

[46] Lu, S. C. Regulation of glutathione synthesis. *Molecular aspects of medicine* **30:**42-59; 2009.

[47] Ruiz, E.; Siow, R. C.; Bartlett, S. R.; Jenner, A. M.; Sato, H.; Bannai, S.; Mann, G. E. Vitamin C inhibits diethylmaleate-induced L-cystine transport in human vascular smooth muscle cells. *Free Radic Biol Med* **34:**103-110; 2003.

[48] Warnatz, H. J.; Schmidt, D.; Manke, T.; Piccini, I.; Sultan, M.; Borodina, T.; Balzereit, D.; Wruck, W.; Soldatov, A.; Vingron, M.; Lehrach, H.; Yaspo, M. L. The BTB and CNC homology 1 (BACH1) target genes are involved in the oxidative stress response and in control of the cell cycle. *J Biol Chem* **286:**23521-23532; 2011.

[49] Loboda, A.; Stachurska, A.; Florczyk, U.; Rudnicka, D.; Jazwa, A.; Wegrzyn, J.; Kozakowska, M.; Stalinska, K.; Poellinger, L.; Levonen, A. L.; Yla-Herttuala, S.; Jozkowicz, A.; Dulak, J. HIF-1 induction attenuates Nrf2-dependent IL-8 expression in human endothelial cells. *Antioxid Redox Signal* **11:**1501-1517; 2009.

[50] Dhakshinamoorthy, S.; Jain, A. K.; Bloom, D. A.; Jaiswal, A. K. Bach1 competes with Nrf2 leading to negative regulation of the antioxidant response element (ARE)-mediated NAD(P)H:quinone oxidoreductase 1 gene expression and induction in response to antioxidants. *J Biol Chem* **280:**16891-16900; 2005.

[51] Sun, J.; Brand, M.; Zenke, Y.; Tashiro, S.; Groudine, M.; Igarashi, K. Heme regulates the dynamic exchange of Bach1 and NF-E2-related factors in the Maf transcription factor network. *Proc Natl Acad Sci U S A* **101:**1461-1466; 2004.

[52] Ogawa, K.; Sun, J.; Taketani, S.; Nakajima, O.; Nishitani, C.; Sassa, S.; Hayashi, N.; Yamamoto, M.; Shibahara, S.; Fujita, H.; Igarashi, K. Heme mediates derepression of Maf recognition element through direct binding to transcription repressor Bach1. *EMBO J* **20:**2835-2843; 2001.

[53] Jyrkkanen, H. K.; Kuosmanen, S.; Heinaniemi, M.; Laitinen, H.; Kansanen, E.; Mella-Aho, E.; Leinonen, H.; Yla-Herttuala, S.; Levonen, A. L. Novel insights into the regulation of antioxidant-response-element-mediated gene expression by electrophiles: induction of the transcriptional repressor BACH1 by Nrf2. *Biochem J* **440:**167-174; 2011.

[54] Sun, J.; Muto, A.; Hoshino, H.; Kobayashi, A.; Nishimura, S.; Yamamoto, M.; Hayashi, N.; Ito, E.; Igarashi, K. The promoter of mouse transcription repressor bach1 is regulated by Sp1 and trans-activated by Bach1. *J Biochem* **130:**385-392; 2001.

[55] Nakayama, M.; Takahashi, K.; Kitamuro, T.; Yasumoto, K.; Katayose, D.; Shirato, K.; Fujii-Kuriyama, Y.; Shibahara, S. Repression of heme oxygenase-1 by hypoxia in vascular endothelial cells. *Biochem Biophys Res Commun* **271:**665-671; 2000.

Figure Legends

Fig. 1. Affymetrix microarray identifies differentially expressed diethylmaleate-responsive Nrf2 target genes in human umbilical vein endothelial cells (HUVEC) adapted to physiological O_2 (5%). (A) Affymetrix transcriptome analysis software computed signaling pathways likely to be affected in EC challenged with diethylmaleate (DEM, 100 μmol. L^{-1}) for 4 h in air or 5% O_2. Molecules from the data set that met the basal/DEM ratio cut-off of >1.2 or <-1.2 and P cut-off of <0.05 were then associated with relevant canonical pathways, with the Nrf2 pathway shown to be the primary pathway induced under both air and 5% O_2 conditions. The volcano plots depict DEM-responsive genes in air (main panel) and 5% O_2 (inset panel) conditions, with the X-axis indicating fold change relative to control and the Y-axis indicating p-value

significance of changes in gene expression. Fewer Nrf2-dependent genes were inducible under 5% O_2, with the primary Nrf2 targets GCLM, xCT and HO-1 induced under both conditions. In the inset, HO-1 is denoted in grey, as separate analyses indicated basal and/or DEM responsiveness may be diminished under 5% O_2. Data derived from independent cultures from 5 different donors. *Gene Abbreviations*: GCLM, glutamate cysteine ligase modifier subunit; SCL7A11/xCT, solute carrier family 7 anionic amino acid transporter light chain; HMOX-1, heme oxygenase-1; NQO1, NAD(P)H quinone oxidoreductase 1; ABCC4, multidrug resistance protein member 4; BACH1, BTB and CNC homology 1, basic leucine zipper transcription factor 1; GSR, glutathione reductase; TXNRD1, thioredoxin reductase 1; SQSTM1, sequestosome 1. (B) HUVEC were loaded with the O_2-sensitive, nanoparticle probe MitoXpress®-INTRA to simultaneously measure O_2 content in the culture medium and cytosol (see Fig. S1). Life-time phosphorescence intensity was measured in an O_2-regulated FLUOstar fluorescence plate reader. HUVEC were maintained under the indicated O_2 level for at least 30 min, at which point cytosolic O_2 levels were stable. Dashed lines highlight ambient O_2 levels most commonly used *in vitro* to mimic *in vivo* levels, with the shaded box denoting 'hypoxic' O_2 levels. (C) Cytosolic O_2 content in HUVEC maintained in air for 60 min before reducing ambient O_2 to 5% (*'physiological normoxia'*) and monitoring cytosolic O_2 levels for a further 60 min. Dissolved O_2 in culture medium was monitored in parallel. (D) Summary of cytosolic and medium O_2 content in HUVEC cultured in air or 5% O_2 for 1 or 5 days. Dashed lines represent the ambient O_2 levels measured during culture of EC in air or 5% O_2.

Fig. 2. Adaptation of HUVEC to 5% O_2 does not alter nuclear Nrf2 expression or ARE binding. EC were cultured in air or adapted to 5% O_2 for 1 or 5 days before treatment with M199 or M199 containing diethylmaleate (DEM, 100µmol.L^{-1}) for 2 h. (A) Representative immunoblot of nuclear Nrf2 protein expression relative to Lamin C. Samples run on same membrane were reorganized for clarity. (B) Nrf2 binding to immobilized ARE consensus sequence on TransAM ELISA plate with values expressed as absorbance at 450nm. Data denote mean ± S.E.M., n = 5-6 different donors, *P<0.05, **P<0.01, ***P<0.001.

Fig. 3. Adaptation of HUVEC to 5% O_2 attenuates induction of HO-1 and NQO1 protein and mRNA expression induced by diethylmaleate. HUVEC were cultured in air or adapted to 5% O_2 for 1 or 5 days before treatment with diethylmaleate (DEM, 100µmol.L^{-1}). Representative immunoblots and densitometric analyses of protein (24 h) or mRNA (4 h) expression of HO-1 (A and B) and NQO1 (C and D). (E) In long-term adaptation experiments, freshly isolated HUVEC were initially cultured in air and 5% O_2 (passage P_0) and then maintained under the same O_2 level for passages P_2-P_3 or switched to either 5% O_2 or air during sequential passages. Representative immunoblot and densitometric analysis of HO-1 expression relative to α-tubulin. Data denote mean ± S.E.M., n = 4-11 different donors, *P<0.05, **P<0.01, ***P<0.001.

Fig. 4. Adaptation of HUVEC to 5% O_2 attenuates HO-1 expression induced by other Nrf2 inducers 4-hydroxynonenal, sulforaphane or DETA NONOate. HUVEC were cultured in air or adapted to 5% O_2 for 1 or 5 days before treatment with 4-hydroxynonenal (HNE, 20μmol.L^{-1}), sulforaphane (SFN, 2.5μmol.L^{-1}) or DETA NONOate (DETA, 500μmol.L^{-1}) versus vehicle (0.08% hexane, 0.01% DMSO or NaOH, respectively). (A-C) Densitometric analysis of HO-1 protein expression in EC challenged with HNE, SFN or DETA. Data denote mean ± S.E.M., n = 4 different donors, **P*<0.05, ***P*<0.01, ****P*<0.001.

Fig. 5. Enhanced Bach1 expression in HUVEC adapted to 5% O_2 underlies decreased induction of HO-1 by diethylmaleate. HUVEC were cultured in air or adapted to 5% O_2 for 1 or 5 days before treatment with M199 or M199 containing DEM (100μmol.L^{-1}) for 4 h or 24 h. (A-B) Representative immunoblot and densitometric analyses of Bach1 protein (24 h) or mRNA (4 h) expression under basal and DEM-stimulated conditions. (C) HUVEC adapted to 5% O_2 for 5 days were transfected with scramble or Bach1 siRNA, and basal and DEM (100μmol.L^{-1}, 24 h) stimulated HO-1 and Bach1 protein expression measured relative to α-tubulin. Data denote mean ± S.E.M., n = 3-7 different donors **P*<0.05, ***P*<0.01, ****P*<0.001.

Fig. 6. Adaptation of HUVEC to 5% O_2 does not affect glutathione synthesis related genes. (A) Basal and diethylmaleate (DEM, 100μmol.L^{-1}, 24 h) stimulated intracellular glutathione (GSH) levels expressed as nmol.mg $protein^{-1}$. (B) Basal and DEM-stimulated mRNA (4 h) expression of cystine-glutamate transporter xCT. (C) Representative immunoblot and densitometric analyses of basal and DEM-stimulated (24 h) glutamate-cysteine ligase modifier subunit (GCLM) protein expression relative to α-tubulin. (D) Bach1 siRNA knockdown has negligible effects on GCLM protein expression. Data denote mean ± S.E.M., n = 5-8 different donors, **P*<0.05, ***P*<0.01, ****P*<0.001.

Fig. 7. Differential regulation of Nrf2-targeted genes in human endothelial cells adapted to physiological O_2 levels encountered *in vivo*. Elevated Bach1 expression in human primary endothelial cells adapted to physiological O_2 (5%) inhibits Nrf2-regulated transcription of HO-1 and NQO1. Notably, long-term adaptation of cells to 5% O_2 does not impair the upregulation of glutathione related genes GCLM and xCT.

Highlights

- Physiological normoxia alters the phenotype and redox signaling in human endothelial cells
- Induction of select Nrf2 target genes, HO-1 and NQO1, is significantly attenuated under 5% O_2
- Diminished HO-1 induction is stimulus independent and reversible upon readaptation of cells to air
- Bach1 mRNA and protein expression are elevated in cells adapted to 5% O_2
- Glutathione synthesis related genes were Bach1 and oxygen insensitive
- Nrf2 confers vascular protection via induction of GCLM and the xCT under physiological normoxia

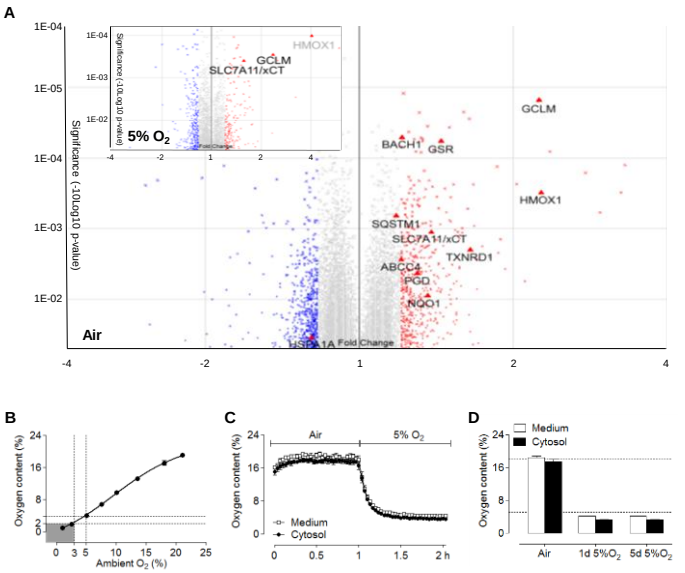

Fig. 1. Chapple *et al.*

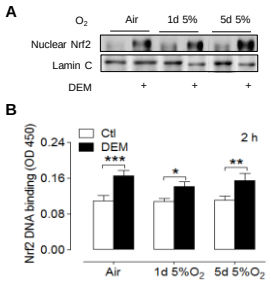

Fig. 2. Chapple *et al.*

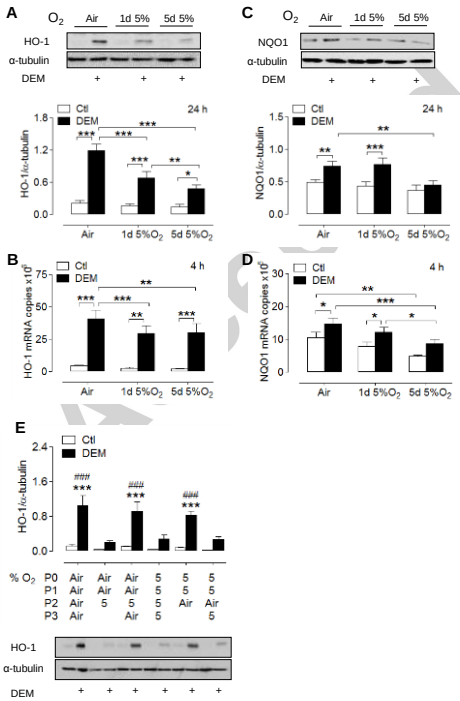

Fig. 3. Chapple *et al*.

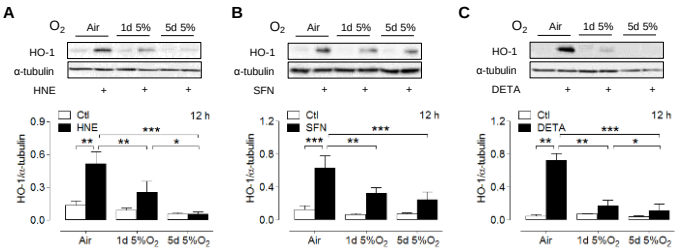

Fig. 4. Chapple *et al.*

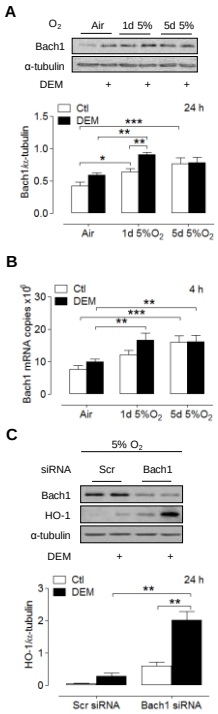

Fig. 5. Chapple et al.

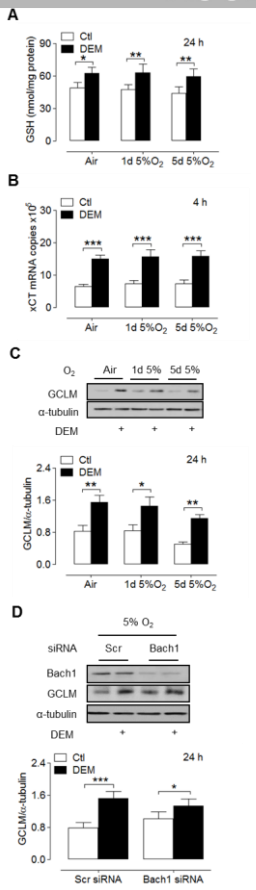

Fig. 6. Chapple *et al.*

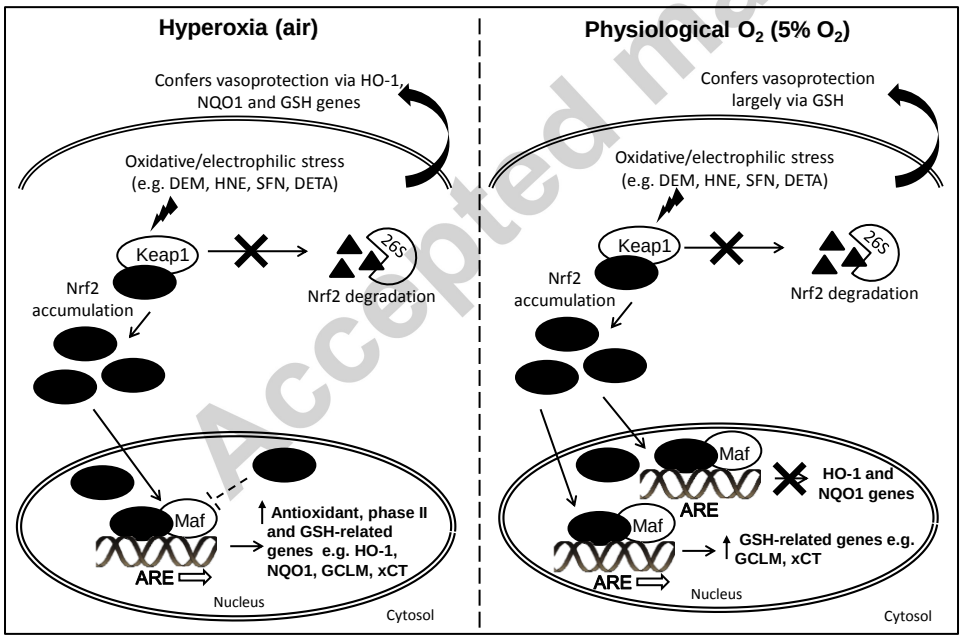

Fig. 7 Chapple *et al.*